SUPPORTING MATERIAL-S1

To attain an accurate fit, the measured reflectance-***R*** had to be corrected by an additional, two-term expression-S1, where R_a and R_b are the calibration parameters (typical values are: R_a=0.70±0.05; R_b=0.00±0.02), introduced to correct the experimental variation in the relative size and position between the sample and the mirror, as well as to account for the small drifts in the intensity and the direction of the light beam (inevitable due to the continues nature of in-situ measurements).

$$(R_b + R_a * \mathbf{R}) \longrightarrow \mathbf{R} \qquad \text{S1.}$$

Yet, thorough parametric analysis revealed a disturbing correlative pattern, expressed by the oscillatory behavior of the R_a; R_b and the d_o; Δ parameter sets. Parametric dependence is demonstrated in figure S1, where R_a; R_b; d_o; Δ and D_o are displayed (thin, dotted lines) against the overall thickness. The derived statistical correlation between mathematically unrelated parameters can be readily explained by the fact that all four parameters (namely, the R_a; R_b; d_o and Δ), affect a similar set of non-distinctive spectral features (i.e., the broadness and intensity). Conversely, D_o, whom dynamic behavior is stable, affects the distinctive peak position feature. This is so since D_o accounts for ~90% of a total scale thickness, a quantity directly related to peak position. Conversely, enlargement in d_o or Δ, cause no peak shift but instigate peak broadening and intensity decrease in ***R***. Analogous effect could be shown for R_a and R_b. There is a deceptive physical reasoning relating the seeming statistical correlation of Δ and d_o. Indeed, both d_o and Δ, represent parameters responsible for "softening" the boundaries of the oxide scale, a phenomenon generally expressed in broadening and intensity decrease of interferences. However, there is also a clear physical difference in origin of the two parameters. This is so since as an intrinsic buffer interface, d_o scale is treated as part of Fresnel reflectance formalism. Conversely, Δ-parameter is a manifestation of scale thickness diversity, treated by simple summation of reflectancies from scale components of various thicknesses. But unlike the Fresnel formalism, summation is valid only for thickness variations sustainable at large-scale areas (>λ), expected to be present due large-scale variations attributed to uneven heating. Though Δ and d_o are physically unrelated, the apparently similar effect on interference shape and intensity, may cause parameter inflation. Clearly, parametric over-definition of the interference shape (but not the position) makes the parameters susceptible to slightest change in the experimental conditions. To minimize the destabilizing effect of multiple parameters, though in a way that would retain the fine description of the system, the consecutive ${}^{i}R_a$; ${}^{i}R_b$ (i-the spectra successive index) were set constant upon averaging ($R_a = \langle {}^{i}R_a \rangle$; $R_b = \langle {}^{i}R_b \rangle$). As illustrated in figure S1 (thick lines), utilization of averaging successfully eliminated the short-period oscillations in d_o and Δ. The prescribed correction technique was proved to be far superior not only in terms of the obvious fit accuracy (increase of >50%), but more importantly, it showed clear improvement in the consistency of the recovered d_o and Δ. As expected, averaging had no impact on D_o.

FIGURE S1

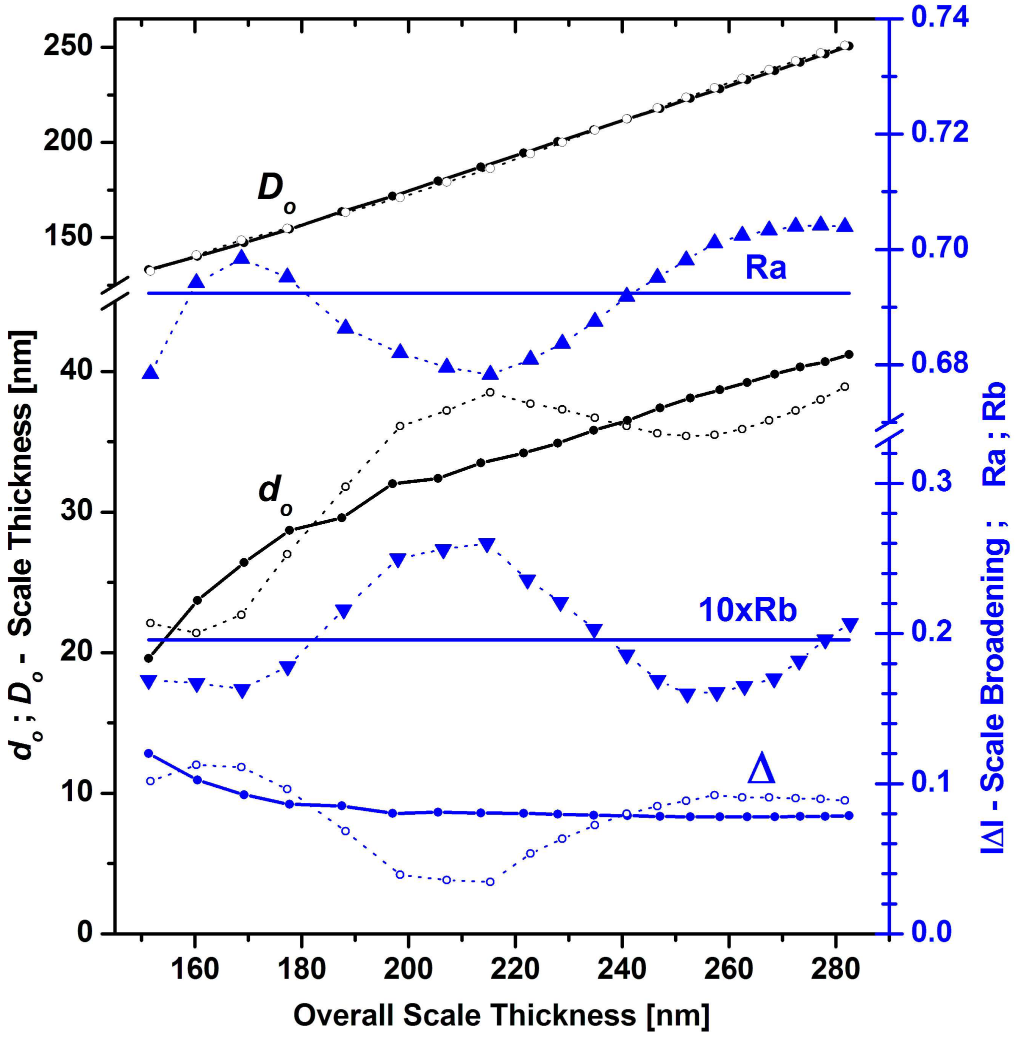

Figure S1: Dynamics of the d_o; Δ and of the R_a; R_b parameters. Presentation of the oscillatory vs. stabilized parameter dependence before (thin, dotted lines) and after (thick, solid lines) the employment of averaging procedure, respectively. Herein, the interactive nature of d_o and Δ (black and blue lines, respectively) and of R_a and R_b (blue lines) in comparison to the stabilized D_o (black line) is demonstrated.

SUPPORTING MATERIAL-S2

As noted previously, spectra of figure 3 were fitted by optimization of *D, d* and Δ. Herein expression for accurateness of $\boldsymbol{R}(D,d,\Delta)$ is presented. Assuming a positive linear dependence between the parameters, the worst-case error is described by the term-S2:

$$\boldsymbol{E_R} = \left|\frac{\partial \boldsymbol{R}}{\partial \boldsymbol{D}}\right| \boldsymbol{E_D} + \left|\frac{\partial \boldsymbol{R}}{\partial \boldsymbol{d}}\right| \boldsymbol{E_d} + \left|\frac{\partial \boldsymbol{R}}{\partial \Delta}\right| \boldsymbol{E}\Delta \qquad \text{S2.}$$

Figure S2 shows the error-bar functional behavior of $\boldsymbol{R}(D,d,\Delta)$ for this case. The analyzed spectrum is the first and the worst (in terms of a random error) of a sequence of in-situ acquired spectra given in figure 3. The derivation which is made numerically, uses an error estimation of ±5% for $\boldsymbol{E_D/D}$, $\boldsymbol{E_d/d}$ and $\boldsymbol{E_\Delta}/\Delta$, each, as obtained from parameter fit of $\boldsymbol{R}(D,d,\Delta)$. It should be mentioned that though some linear dependency is evident and been discussed comprehensively in section S1, the extensiveness or the exact type of error dependency is not clear. However, as some indications imply (see discussion in S1), there is systematic negative error functionality between the derived $\boldsymbol{D}$ and $\boldsymbol{d}$, which make the actual $\boldsymbol{E_R}$ estimation much lower. We did not analyze this aspect further since our worst-case estimate gave an adequate result.

FIGURE S2

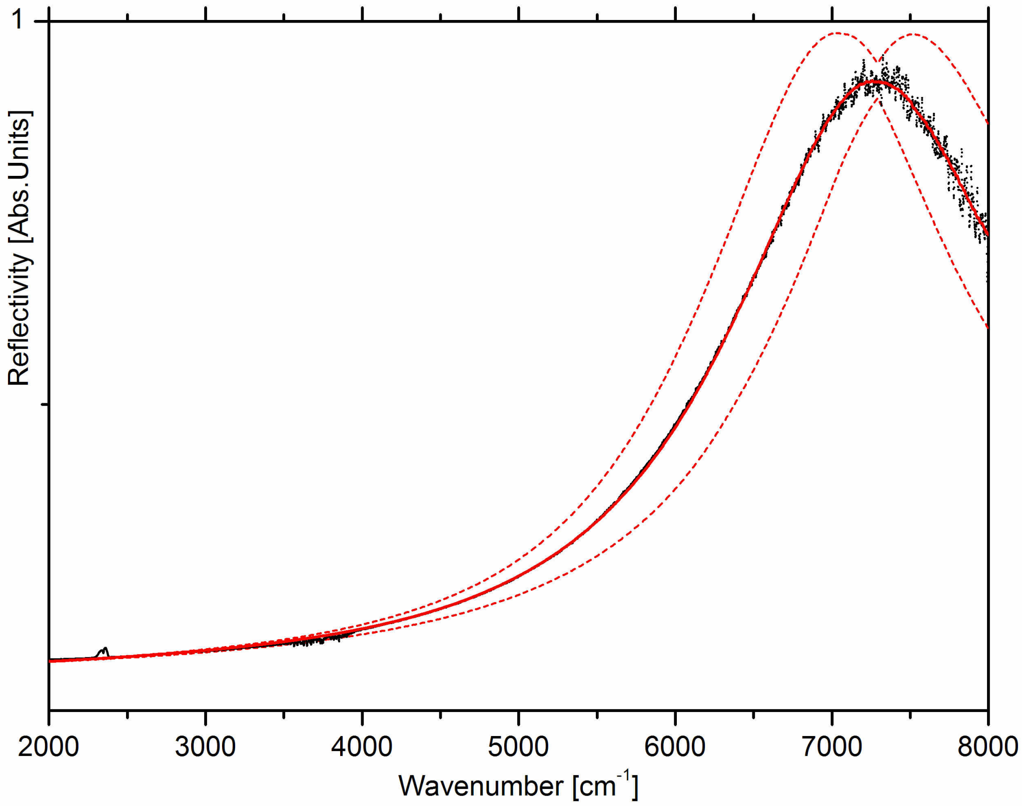

Figure S2: The error-bars for $\boldsymbol{R(D,d,\Delta)}$. Calculation is based on the assumption of positive linear dependence between the $\boldsymbol{D}$, $\boldsymbol{d}$ and Δ embodying ±5% error each.

SUPPORTING MATERIAL-S3

Comparative results of kinetic modelization are shown for Uranium sample, oxidized at 140°C. Herein, the proposed multi-level parabolic model is referenced against the: a) Classic parabolic model of differential equation 5 and b) Inverse-logarithmic time dependence discussed in Theoretical Background section and shown in equation s3 (*K* and *a* are composite rate constants). Fits for all three models are presented in figure s3 and the statistics is given in table-s3.

$$x = [x_o^{-1} - K * ln(1 + a * t)]^{-1} \qquad \textbf{S3.}$$

Markedly, the inverse-logarithmic kinetic model is inferior, even in comparison to the classic parabolic model. Though, the classic parabolic kinetics is clearly outperformed by the much superior multi-level parabolic model presented in current study.

TABLE S3:

Statistical comparison of the multi-level, classic parabolic and the inverse-logarithmic models.

Model Type (→) **Fit Statistics (↓)**	**Two-level Parabolic**	**Classic Parabolic**	**Inverse-Logarithmic**
# of Parameters	**3***	**2***	**3***
Reduced Error : χ^2	**0.157**	**5.238**	**18.259**
Regression : R^2	**0.99984**	**0.99721**	**0.99083**

* This includes fitting of the x_o (initial x at $t=t_o$) variable.

FIGURE S3

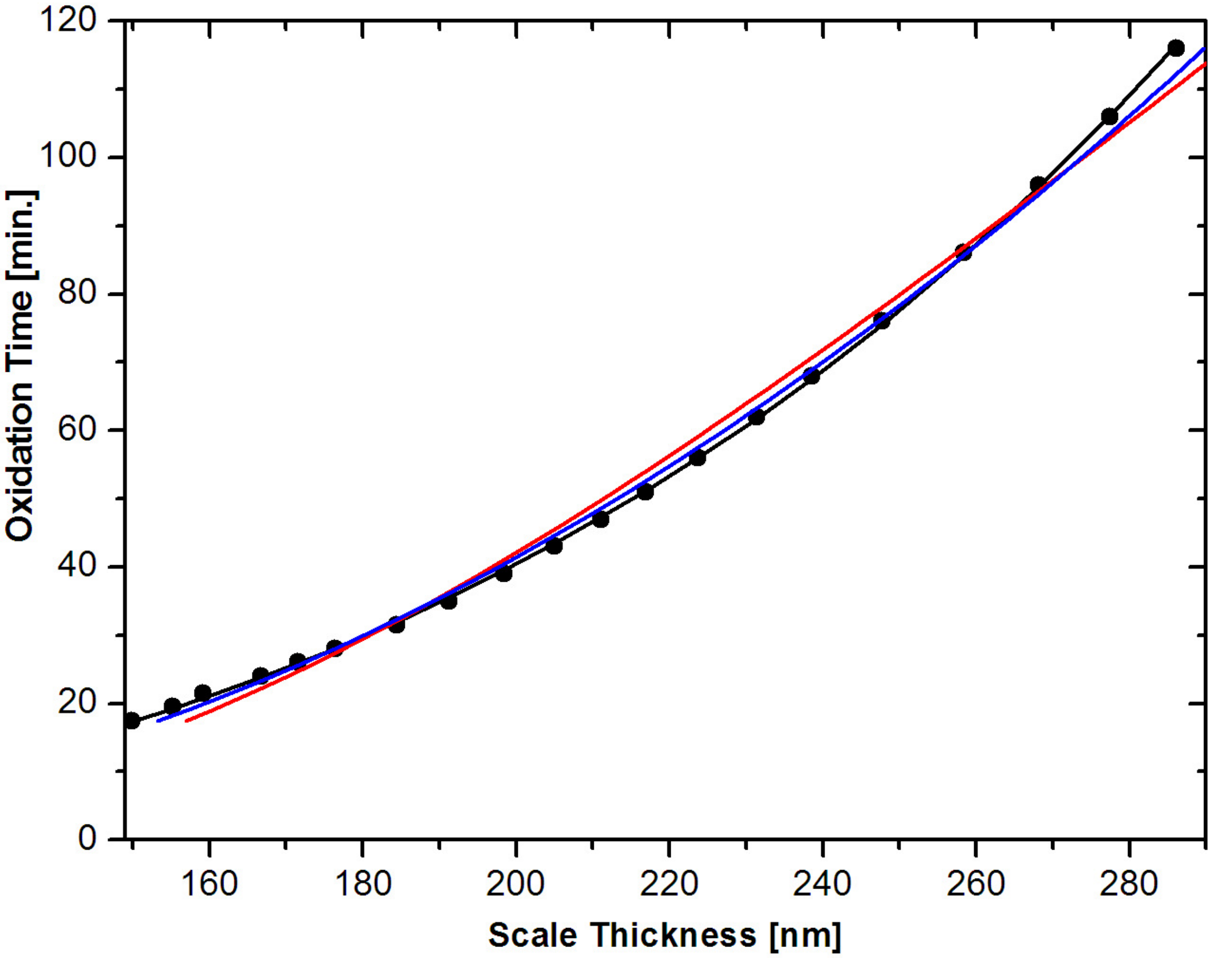

Figure S3: Fitting of the multi-level (black), classic parabolic (blue) and the inverse-logarithmic (red) models.